SPANDIDOS PUBLICATIONS

MOLECULAR MEDICINE REPORTS 19: 4109-4118, 2019

Growth differentiation factor 11 is involved in isoproterenol-induced heart failure

XIU-JING ZHANG[1], HUA TAN[1], ZHI-FANG SHI[2], NA LI[1], YING JIA[1] and ZHE HAO[1]

The [1]First and [2]Second Departments of Cadres Health Care,
The Third Hospital of Shijiazhuang, Shijiazhuang, Hebei 050011, P.R. China

Received June 13, 2018; Accepted February 2, 2019

DOI: 10.3892/mmr.2019.10077

Abstract. The present study aimed to investigate the potential effects of growth differentiation factor 11 (GDF11) on isoproterenol (ISO)-induced heart failure (HF) and identify the underlying molecular mechanisms. A rat model of HF was induced *in vivo* by intraperitoneally administering ISO (5 mg/kg/day) for 7 days. After 4 weeks following establishment of the HF model, hemodynamic analysis demonstrated that ISO induced a significant increase in the left ventricular end-diastolic pressure and a decrease in the left ventricular systolic pressure and maximum contraction velocity. The plasma levels of myocardial injury markers, including lactate dehydrogenase (LDH), creatine kinase (CK), CK-muscle/brain which were determined using the corresponding assay kits and plasma brain natriuretic peptide which was detected by an ELISA kit, an important biomarker of HF, increased following ISO treatment. Furthermore, levels of GDF11 expression and protein, which were estimated using reverse transcription-quantitative polymerase chain reaction and an ELISA kit in plasma and western blotting in the heart tissue, respectively, significantly increased following ISO treatment. To demonstrate the effects of ISO on GDF11 production in cardiomyocytes, H9C2 cells (a cardiomyoblast cell line derived from embryonic rat heart tissue) were treated with ISO (50 nM) for 24 h *in vitro*; it was revealed that GDF11 protein and mRNA expression levels significantly increased following ISO treatment. In addition, recombinant GDF11 (rGDF11) administered to ISO-treated H9C2 cells resulted in decreased proliferation, which was detected via a CCK-8 assay, and increased LDH levels and cell apoptosis of cells, which was determined using Caspase-3 activity and Hoechst 33258 staining. Additionally, rGDF11 increased the levels of reactive oxygen species and malondialdehyde due to the upregulation of nicotinamide adenine dinucleotide phosphate oxidase 4 (Nox4) following rGDF11 treatment. Conversely, GDF11 knockdown reduced ISO-induced apoptosis by inhibiting oxidative stress injury. The results suggested that GDF11 production was upregulated in ISO-induced rats with HF and in ISO-treated H9C2 cells, and that rGDF11 treatment increased ISO-induced oxidative stress injury by upregulating Nox4 in H9C2 cells.

Correspondence to: Dr Xiu-Jing Zhang, The First Department of Cadres Health Care, The Third Hospital of Shijiazhuang, 15 Sports South Street, Shijiazhuang, Hebei 050011, P.R. China
E-mail: xiujingzhang818283@126.com

Key words: growth differentiation factor 11, heart failure, isoproterenol, oxidative stress, nicotinamide adenine dinucleotide phosphate oxidase 4

Introduction

Advancements in clinical care and increased public awareness have been made; however, heart failure (HF) remains a leading cause of morbidity and mortality globally (1). HF is considered as the terminal pathological manifestation of various cardiovascular diseases, including coronary artery disease, hypertension and valvular disease. HF frequently leads to cardiac overload or myocardial injury, which ultimately results in an insufficient blood supply to meet the metabolic demands of the body. HF is pathologically characterized by cardiomyocyte loss, leading to cardiac apoptosis, hypertrophy, fibrosis and dysfunctional ventricular remodeling, which impairs the contraction and/or relaxation of the ventricles, and reduces cardiac ejection fraction (2,3). Numerous mechanisms have been hypothesized to contribute to the development of HF, including impaired calcium homeostasis, increased reactive oxygen species (ROS) concentration, accelerated cardiomyocyte apoptosis and autophagy, and renin-angiotensin-system and sympathetic nerve activation (4-8); however, understanding of the precise mechanisms underlying the pathogenesis of HF remains limited.

The transforming growth factor β (TGF-β) superfamily, including TGF-β1-3, bone morphogenetic proteins (BMPs), growth differentiation factors (GDFs), activins and nodal-associated proteins (9), has been proposed to serve important roles in the progression of HF (10,11). Of these factors, TGF-β1 is the most widely studied, and serves various roles in HF that may affect cell growth, apoptosis and differentiation, including promotion of collagen and matrix protein production, maintenance of fibroblast viability and inhibition of collagen degradation (12,13). GDF15, a member of the TGF-β superfamily, is a potential diagnostic marker for HF; increased circulating levels of GDF15 are associated with the severity and progression of HF (14). A recent study reported that the expression levels of BMP9, another member of the TGF-β

superfamily, were increased in patients with HF; furthermore, increasing BMP9 activity by treatment with recombinant (r)BMP9 or inhibiting the BMP9 receptor attenuated cardiac fibrosis, and improved cardiac function in HF (15).

GDF11, also known as BMP11, is a member of the TGF-β superfamily and contributes to the regulation of cell growth and differentiation in embryonic and adult tissues (16). Furthermore, it serves important roles in diverse biological processes and diseases (17-19). The biological role of GDF11, particularly in the cardiovascular system, is heavily debated. Loffredo *et al* (20) reported that circulating levels of GDF11 reduced with aging, and restoration of GDF11 expression in older mice using heterochronic parabiosis reversed age-associated cardiac hypertrophy via cardiomyocyte regeneration, and downregulation of brain natriuretic peptide (BNP) and atrial natriuretic peptide. Data from large human cohorts demonstrated that increased levels of GDF11 expression are associated with a reduced risk of cardiovascular events and mortality in patients with stable ischemic heart diseases (21). Conversely, Smith *et al* (22) reported that restoring levels of GDF11 in old mice did not improve aging-associated pathological cardiac hypertrophy; however, high levels of GDF11 induced neonatal rat ventricular myocyte hypertrophy. Schafer *et al* (23) used a specifically-developed liquid chromatography-tandem mass spectrometry assay to quantify GDF11 expression, and revealed that GDF11 levels did not decrease with aging in healthy men, and that individuals with increased GDF11 levels were more likely to be frail with diabetes or prior cardiac conditions than those with reduced GDF11 levels. Thus, the role of GDF11 in cardiovascular diseases remains controversial. Further investigation is required to validate GDF11 as a therapeutic target in the treatment of cardiovascular diseases, particularly HF. The present study aimed to determine the effects of GDF11 on isoproterenol (ISO)-induced HF and investigate the underlying molecular mechanisms.

Materials and methods

Animals and treatment. Twelve male Sprague-Dawley rats, aged 8-weeks-old and weighing 220-260 g, were supplied by Beijing Vital River Laboratory Animal Technology Co., Ltd. (Beijing, China). The rats were housed at constant temperature (22±2˚C) and humidity (60%) under a 12-h light/dark cycle, and provided with *ad libitum* access to water and food for 1 week prior to initiation of the experiment. All animal care and experimental procedures were performed according to the Guide for the Care and Use of Laboratory Animals of the US National Institutes of Health (National Institutes of Health publication no. 85-23) (24). The present study was approved by the Ethics Committee of Third Hospital of Shijiazhuang [Shijiazhuang, China; approval no. 054(2018)].

Following an acclimatization period of one week, the rats were randomly assigned to control and ISO groups (n=6). Rats in the ISO and control groups were intraperitoneally administered ISO (5 mg/kg) or equal volume of saline daily for one week to induce HF as previously described (25).

Hemodynamic measurement. After 4 weeks following successful establishment of the model of HF, the rats were intraperitoneally anesthetized using urethane (1.2 g/kg). To evaluate left ventricular function, a heparin-filled catheter connected to a pressure transducer (Chengdu Taimeng Technology Co., Ltd., Chengdu, China) was inserted into the left ventricle from the right carotid artery to measure hemodynamic parameters, including left ventricular systolic pressure (LVSP), left ventricular end-diastolic pressure (LVEDP), heart rate (HR), maximum contraction velocity ($+dp/dt_{max}$) and maximum relaxation velocity ($-dp/dt_{max}$). Following recording, rats were sacrificed, and their hearts were immediately dissected and frozen at -80˚C for subsequent experimentation. Additionally, blood was collected from the right common carotid artery and centrifuged at 1,370 x g at 4˚C for 10 min to obtain plasma, which was collected and stored at -80˚C for subsequent analysis.

Biochemical analysis. Plasma lactate dehydrogenase (LDH), creatine kinase (CK) and CK-muscle/brain (CK-MB) levels were determined using the corresponding assay kits (cat. nos. A020-2, A032, H197, respectively; Nanjing Jiancheng Bioengineering Institute, Nanjing, China) according to the manufacturer's protocols.

Measurement of plasma BNP and GDF11. The plasma levels of BNP (cat. no. JYM00013; Wuhan Colorful Gene Biological Technology, Wuhan, China) and GDF11 (cat. no. E-EL-R0463c; Elabscience Biotechnology Co., Ltd, Wuhan, China) were determined using the corresponding assay kits according to the manufacturer's protocols.

Cell culture and treatment. H9C2 rat cardiac myoblasts, a cardiomyoblast cell line derived from the heart tissue of embryonic rats (Chinese Academy of Sciences Cell Bank, Shanghai, China), were cultured in Dulbecco's Modified Eagle's medium (DMEM; Gibco; Thermo Fisher Scientific, Inc., Waltham, MA, USA) supplemented with 10% fetal bovine serum (HyClone; GE Healthcare, Logan, UT, USA) and 1% penicillin-streptomycin (Invitrogen; Thermo Fisher Scientific, Inc.) at 37˚C in 5% CO_2. H9C2 cells were categorized into three groups based on treatment: i) Control group (cells were cultured in DMEM for 24 h and then treated with saline at 37˚C for 24 h); ii) ISO group (cells were cultured in DMEM for 24 h and then treated with 10 μM ISO at 37˚C for 24 h); and iii) ISO + rGDF11 group [cells were pre-incubated with different concentrations (0.5, 5 or 50 nM) of rGDF11 protein (cat. no. 1958-GD; R&D Systems, Inc., Minneapolis, MN, USA) (22) at 37˚C for 24 h and then treated with 10 μM ISO at 37˚C for 24 h].

GDF11 silencing using small interfering RNA (siRNA). H9C2 cells were inoculated in 6-well culture plates and transfections were performed using Lipofectamine® 2000 (Invitrogen; Thermo Fisher Scientific, Inc.) according to the manufacturer's protocols. Specific siRNA against GDF11 (5'-GCCAGU GCGAGUACAUGUUTTdTdT-3') and scrambled siRNA (5'-UUCUCCGAACGUGUCACGUdTdT-3'; negative control) were obtained from Ambion (cat. no. AM16708; Thermo Fisher Scientific, Inc.). For each reaction, 5 μl of siRNA, 5 μl of Lipofectamine 2000 and 95 μl of Opti-MEM™ reduced-serum medium (Invitrogen; Thermo Fisher Scientific,

Inc.) were mixed at room temperature followed by incubation at 37˚C for 20 min. Opti-MEM (800 μl) was subsequently added drop-wise to each well. H9C2 cells were then added to the resultant mixture. Following transfection for 6 h, the cell culture medium was replaced and cells were further incubated at 37˚C for 24 h prior to treatment with ISO.

CCK-8 assays. The proliferation of H9C2 cells cultured at a density of $1x10^4$ cells/well in 96-well plates was measured using the Cell Counting Kit-8 (CCK-8; Dojindo Molecular Technologies, Inc., Kumamoto, Japan) according to the manufacturer's protocols. The absorbance of the cells at 450 nm was determined using a microplate reader and normalized to that of the control group.

LDH activity. The extent of cellular injury was monitored by LDH release. H9C2 cells were cultured at a density of $1x10^6$ cells/well in 6-well plates. Following treatment, the culture medium was analyzed to determine LDH activity using a LDH assay kit (Nanjing Jiancheng Bioengineering Institute) with a microplate reader.

Caspase-3 activity. Caspase-3 activity was determined to investigate the apoptosis of cells. Following treatment, H9C2 cells cultured at a density of $1x10^6$ cells/well in 6-well plates were homogenized using 50 mM of potassium phosphate buffer. Following centrifugation at 10,000 x g at 4˚C for 10 min, the supernatant was analyzed using the caspase-3 activity kit (Beyotime Institute of Biotechnology, Shanghai, China) according to the manufacturer's protocols. Briefly, 50 μl supernatant was mixed with 10 μl caspase-3 substrate Ac-DEVD-pNA and 40 μl buffer solution, and then incubated at 37˚C for 2 h, and absorbance at 450 nm was measured, reflecting cleavage of the colorimetric substrate. Finally, values were normalized to those of the control group.

Hoechst 33258 staining. Apoptotic cell death was determined by Hoechst 33258 (Sigma-Aldrich; Merck KGaA, Darmstadt, Germany) staining. In brief, H9C2 cells were cultured at a density of $1x10^6$ cells/well in 6-well plates. Following treatment, the cells were fixed with 1 ml of 4% paraformaldehyde at 37˚C for 30 min. Then, the cells were incubated in 1 ml PBS containing 10 μM Hoechst 33258 at 37˚C for 30 min and observed using fluorescence microscopy (Olympus Corporation, Tokyo, Japan) from five random fields (x200). Normal nuclei stained blue and apoptotic nuclei were identified as condensed or fragmented nuclei stained bright blue. The rate of apoptosis was calculated as follows: Apoptotic rate=No. of apoptotic cells/Total no. of cells x100.

Detection of intracellular ROS. Intracellular ROS generation was estimated using dihydroethidium (DHE; Sigma-Aldrich; Merck KGaA) fluorescent staining. Briefly, following treatment as aforementioned, H9C2 cells cultured at a density of $1x10^4$ cells/well in 96-well plates were washed with PBS and incubated with DHE (10 μM) at 37˚C for 30 min in the dark. Then, DHE was removed by washing with PBS, and the fluorescence intensity was measured using a fluorescence plate reader (Tecan Infinite M200, Mannedorf, Switzerland) at excitation/emission wavelength of 488/610 nm, respectively. The values were normalized to those of the control group.

Determination of intracellular malondialdehyde (MDA). Following treatment as aforementioned, H9C2 cells cultured at a density of $1x10^6$ cells/well in 6-well plates were homogenized using 50 mM potassium phosphate buffer. Following centrifugation at 10,000 x g at 4˚C for 10 min, the MDA concentration of the supernatant was analyzed using an MDA assay kit (Nanjing Jiancheng Bioengineering Institute) according to the manufacturer's protocols and the optical density (OD) was measured at 532 nm using a microplate reader. The obtained values were standardized to total protein content, which was determined via a bicinchoninic acid (BCA) protein assay kit.

Western blot analysis. Protein extracted from heart tissues or H9C2 cells was quantified using a BCA protein assay kit. Proteins (50 μg) were separated via 10% SDS-PAGE, transferred to polyvinylidene difluoride membranes, and blocked using 5% non-fat milk at room temperature for 1 h. Subsequently, the membranes were incubated overnight at 4˚C with the following primary antibodies: Anti-B-cell lymphoma 2 (Bcl-2; 1:1,000; cat. no. 3498; Cell Signaling Technology, Inc., Danvers, MA, USA); anti-Bcl-2-associated X protein (Bax; 1:1,000; cat. no. 5023; Cell Signaling Technology, Inc.); anti-nicotinamide adenine dinucleotide phosphate oxidase 2 (Nox2; 1:1,000; cat. no. 19013-1; ProteinTech Group, Inc., Chicago, IL, USA); anti-Nox4 (1:1,000; cat. no. 14347-1; ProteinTech Group, Inc.); anti-GDF11 (1:1,000; cat. no. AF1958; R&D Systems, Inc.) and anti-GAPDH as an internal control (1:2,000; cat. no. 10494-1; ProteinTech Group, Inc.). Following three washes in TBS-Tween 20 (0.5 ml/l), the membranes were incubated with horseradish peroxidase-conjugated secondary antibodies (1:1,000; cat. no. A0208; Beyotime Institute of Biotechnology) at room temperature for 1 h. Target bands were detected using the SuperSignal West Pico Chemiluminescent Substrate (Pierce; Thermo Fisher Scientific, Inc.), and band intensity was quantified using ImageJ 1.48i software (National Institutes of Health, Bethesda, MD, USA). The experiment was repeated three times.

Reverse transcription-quantitative polymerase chain reaction (RT-qPCR). Total RNA was extracted from heart tissues or H9C2 cells using TRIzol® reagent (Invitrogen; Thermo Fisher Scientific, Inc.) and 1 μg RNA was subjected to reverse transcription using first-strand cDNA synthesis kit (Promega Corporation, Madison, WI, USA) according to the manufacturer's protocols. The temperature protocol was as follows: 42˚C for 30 min and 85˚C for 5 min. Real-time PCR analysis was performed with the ABI 7500 FAST system, using an SYBR® Green RT-PCR kit (Toyobo Life Science, Osaka, Japan) according to the manufacturer's protocols. The thermocycling conditions consisted of an initial, single cycle of 2 min at 94˚C, followed by 40 cycles of 15 sec at 94˚C, 20 sec at 60˚C and 30 sec at 70˚C. As an internal control, β-actin primers were used for RNA template normalization. All PCRs were performed in triplicate. The primers used to determine gene expression were as follows: Rat GDF11, forward 5'-TGGGGAGCAGGCAAGGGGTAG-3', reverse,

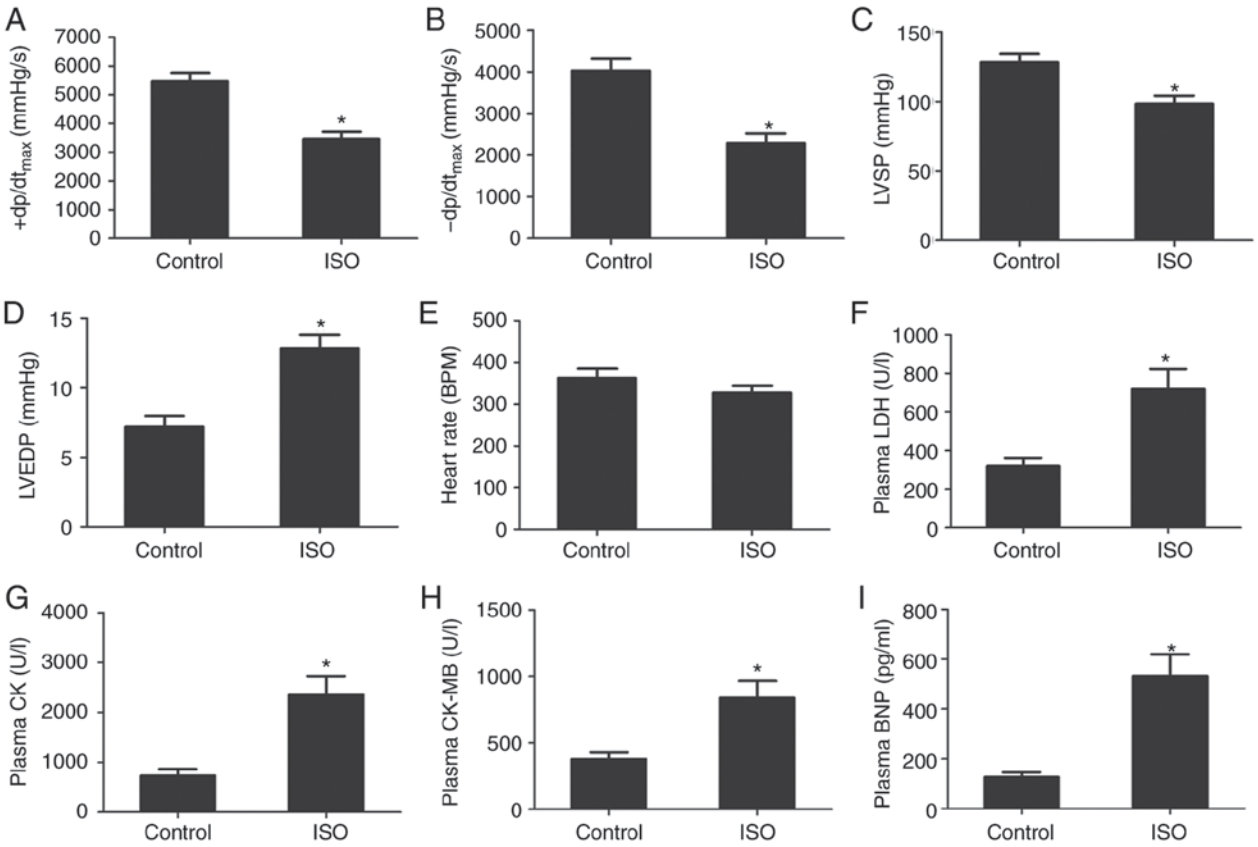

Figure 1. ISO induces heart failure in rats. (A) +dp/dt_{max}, (B) -dp/dt_{max}, (C) LSVP, (D) LVEDP and (E) heart rate of rats following control or ISO treatment. (F) LDH, (G) CK, (H) CK-MB and (I) BNP expression levels in plasma following control or ISO treatment. Data are presented as the mean ± standard error of the mean. *P<0.01 vs. control group. BNP, brain natriuretic peptide; CK-MB, creatine kinase muscle/brain; ISO, isoproterenol; LDH, lactate dehydrogenase; LSVP, left ventricular systolic pressure; LVEDP, left ventricular end-diastolic pressure; +dp/dt_{max}, maximum contraction velocity; -dp/dt_{max}, maximum relaxation velocity.

5'-TGCCCGTGGTAAGTGCTCAGAA-3'; and rat β-actin, forward 5'-TACCACATCCAAGGAAGGCAGCA-3' and reverse, 5'-TGGAATTACCGCGGCTGCTGGCA-3'. Fold changes in GDF11 expression normalized to β-actin expression were calculated using the $2^{-\Delta\Delta Cq}$ method (26).

Statistical analysis. Data were presented as the mean ± standard error of the mean. Statistical analysis was performed using SPSS version 17.0 (SPSS, Inc., Chicago, IL, USA). Comparisons between two rat groups were conducted using Student's t-tests. Comparisons between >2 groups were performed using one-way analyses of variance followed by a Tukey's test. P<0.05 was considered to indicate a statistically significant difference.

Results

ISO induces HF in rats. The results of hemodynamic analysis revealed that ISO treatment induced a significant increase in LVEDP, and a decrease in LVSP and ± dp/dt_{max} in the ISO group compared with the control group (Fig. 1A-D). A significant difference in HR was not observed; however, the mean value was markedly lower in the ISO group than in the control group (Fig. 1E). The results indicated that ISO treatment induced cardiac dysfunction in rats.

ISO-induced HF was associated with increased plasma levels of myocardial injury markers, including LDH, CK and CK-MB. Compared with the control group, the plasma levels of LDH, CK and CK-MB increased significantly following ISO treatment (Fig. 1F-H). Additionally, plasma BNP levels, an important biomarker of HF, were significantly elevated following ISO treatment compared with the control group (Fig. 1I). These findings suggested that ISO treatment induced HF in rats.

ISO increases the generation of GDF11 in vivo and in vitro. As presented in Fig. 2A-C, the levels of GDF11 protein and mRNA expression were significantly increased in the heart tissues of ISO-treated rats compared with in the control group; however, the mean plasma GDF11 levels were markedly unchanged. Additionally, to demonstrate the effects of ISO on GDF11 production in cardiomyocytes, H9C2 cells were treated with ISO for 24 h. As presented in Fig. 2D and E, the levels of GDF11 protein and mRNA expression in H9C2 cells were significantly increased following ISO treatment compared with the control.

GDF11 aggravates ISO-induced damage in H9C2 cells. To investigate the roles of GDF11 in ISO-treated H9C2 cells, rGDF11 was used in the following experiments. rGDF11 significantly reduced the proliferation (Fig. 3A) and increased LDH levels (Fig. 3B) in ISO-treated H9C2 cells in a dose-dependent manner compared with ISO treatment only; 50 nM rGDF11 was selected for use in subsequent experiments.

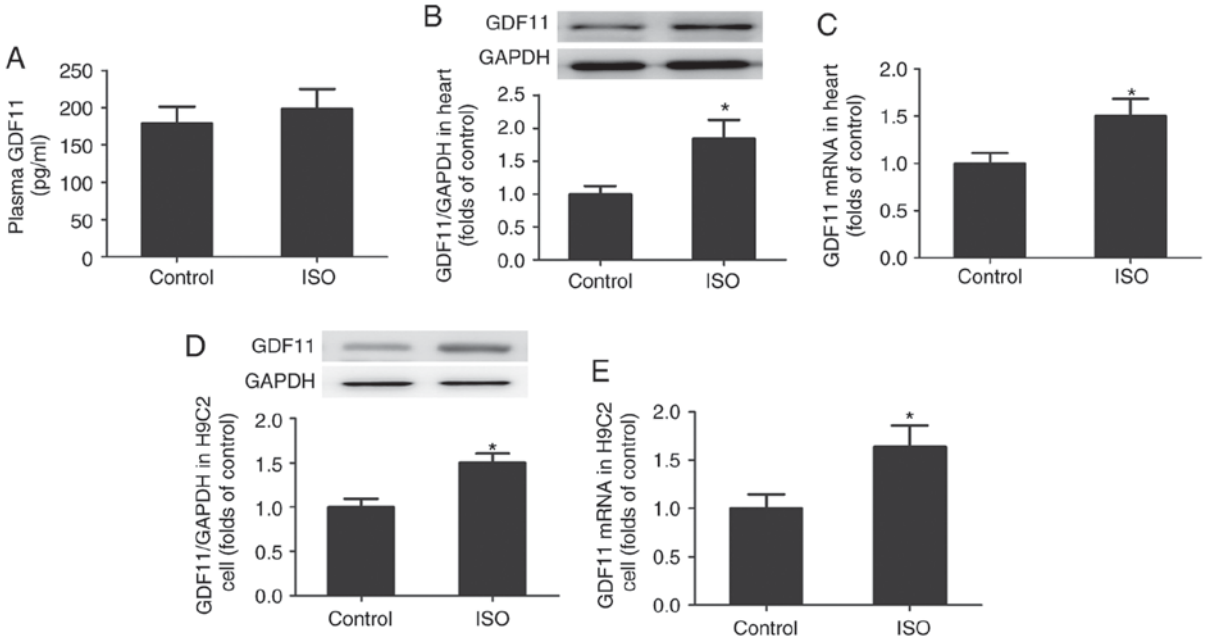

Figure 2. ISO increases the production of GDF11 *in vivo* and *in vitro*. (A) Levels of GDF11 in plasma following control and ISO treatment determined by ELISA. Levels of GDF11 (B) protein and (C) mRNA expression in heart tissues from control- and ISO-treated rats as determined via western blotting and RT-qPCR, respectively. Levels of GDF11 (D) protein and (E) mRNA expression in control- and ISO-treated H9C2 cells as determined via western blotting and RT-qPCR, respectively. Data are presented as the mean ± standard error of the mean. *P<0.05 vs. control group. GDF11, growth differentiation factor 11; ISO, isoproterenol; RT-qPCR, reverse transcription-quantitative polymerase chain reaction.

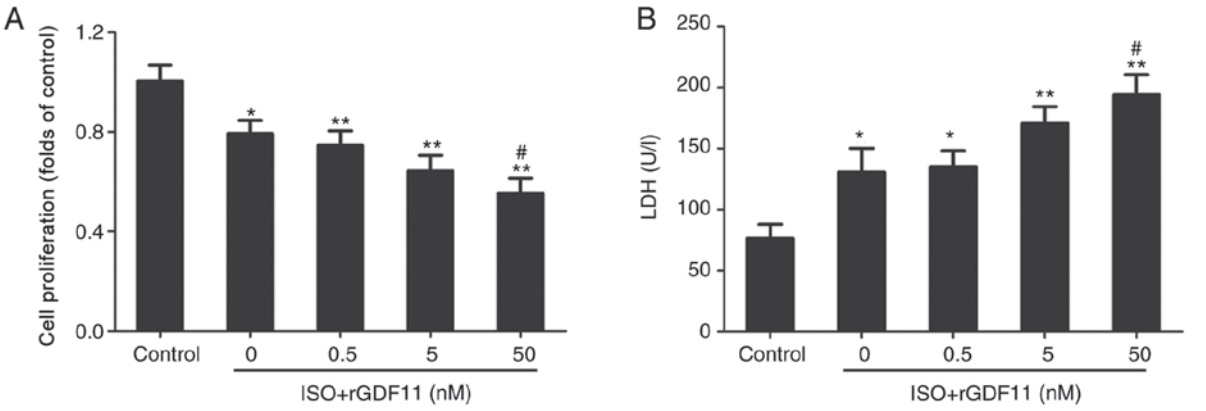

Figure 3. GDF11 reduces the proliferation and increases LDH release of ISO-treated H9C2 cells in a dose-dependent manner. (A) Proliferation of H9C2 cells was measured using a Cell Counting Kit-8 assay. (B) LDH levels in H9C2 cells. Data are presented as the mean ± standard error of the mean. *P<0.05, **P<0.01 vs. control group; #P<0.05 vs. ISO group. rGDF11, recombinant growth differentiation factor 11; ISO, isoproterenol; LDH, lactate dehydrogenase.

It was revealed that, compared with ISO treatment, 50 nM rGDF11 significantly reduced the proliferation (Fig. 4A), and increased the LDH release (Fig. 4B) and apoptosis of H9C2 cells, represented by the increase in Bax/Bcl-2 protein expression, caspase-3 activity and apoptotic rate in Hoechst 33258 staining (Fig. 4C-G).

GDF11 increases ISO-induced oxidative stress by upregulating Nox4 in H9C2 cells. ISO treatment often induces oxidative stress injury that is reflected by increased ROS and MDA concentrations (27). As presented in Fig. 5A and B, the concentrations of ROS and MDA were significantly increased in the ISO group compared with in the control group. rGDF11 in addition to ISO treatment further increased ROS and MDA concentrations compared with ISO treatment only.

To further investigate the potential molecular mechanisms underlying ISO-induced HF, the expression levels of the Nox subunits, Nox2 and Nox4, in H9C2 cells were determined via western blot analysis (Fig. 5C). The results revealed that Nox4 protein levels were significantly increased in the ISO group compared with in the control group and were further upregulated following rGDF11 treatment; however, no significant alterations in Nox2 expression were observed (Fig. 5D and E).

GDF11 knockdown alleviates ISO-induced apoptosis by inhibiting oxidative stress injury. To further investigate the effects of GDF11 on ISO-treated H9C2 cells, GDF11 was downregulated by siRNA-mediated knockdown (Fig. 6A). Compared with the scrambled siRNA group, silencing of GDF11 significantly increased the proliferation (Fig. 6B), and

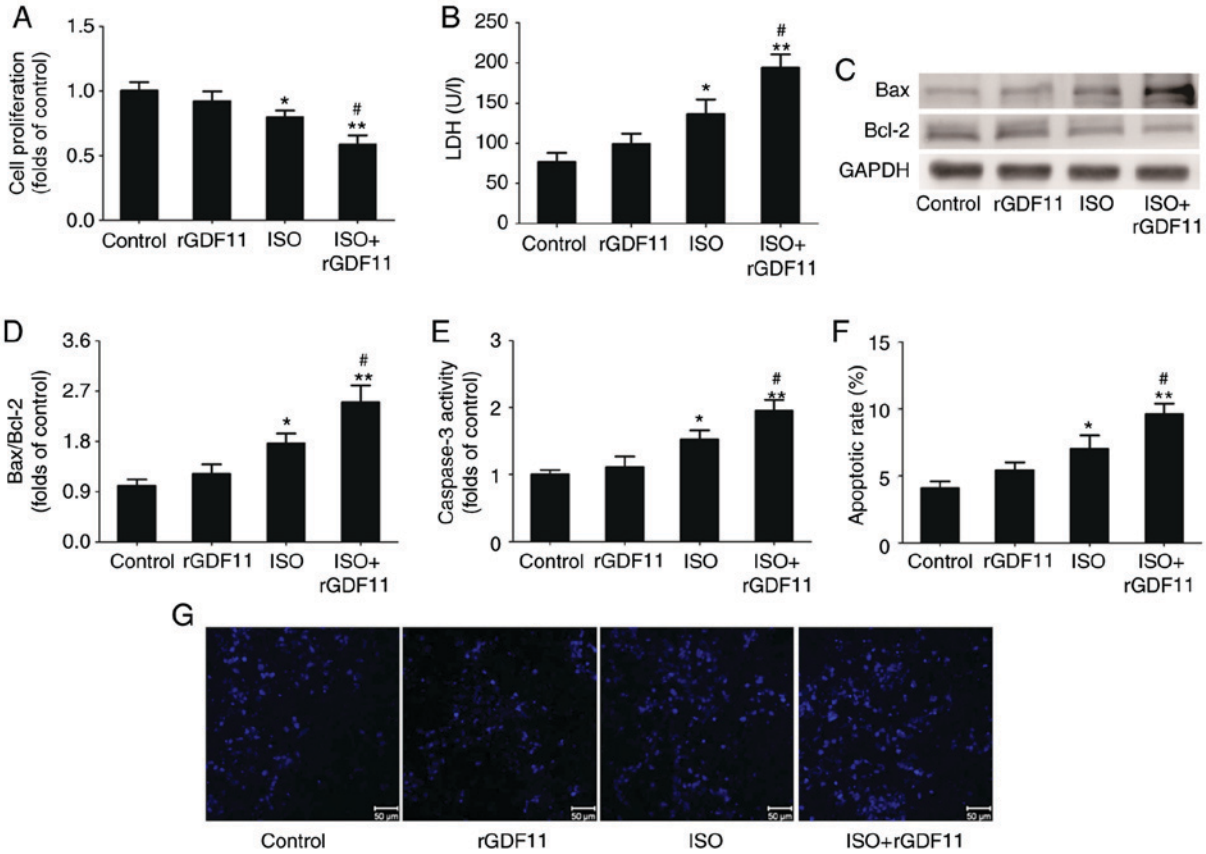

Figure 4. GDF11 aggravates ISO-induced cell damage in H9C2 cells. (A) Proliferation of H9C2 cells was measured using a Cell Counting Kit-8 assay. (B) Levels of LDH release from H9C2 cells. (C) Representative western blot and (D) quantitative analyses of Bax and Bcl-2 protein expression in treated H9C2 cells. (E) Caspase-3 activity in H9C2 cells. (F) Quantitative analysis and (G) representative images of apoptotic H9C2 cells stained with Hoechst 33258. Scale bar, 50 μm. Data are presented as the mean ± standard error of the mean. *P<0.05, **P<0.01 vs. control group; $^{\#}$P<0.05 vs. ISO group. Bcl-2, B-cell lymphoma 2; Bax, Bcl-2-associated X protein; rGDF11, recombinant growth differentiation factor 11; ISO, isoproterenol.

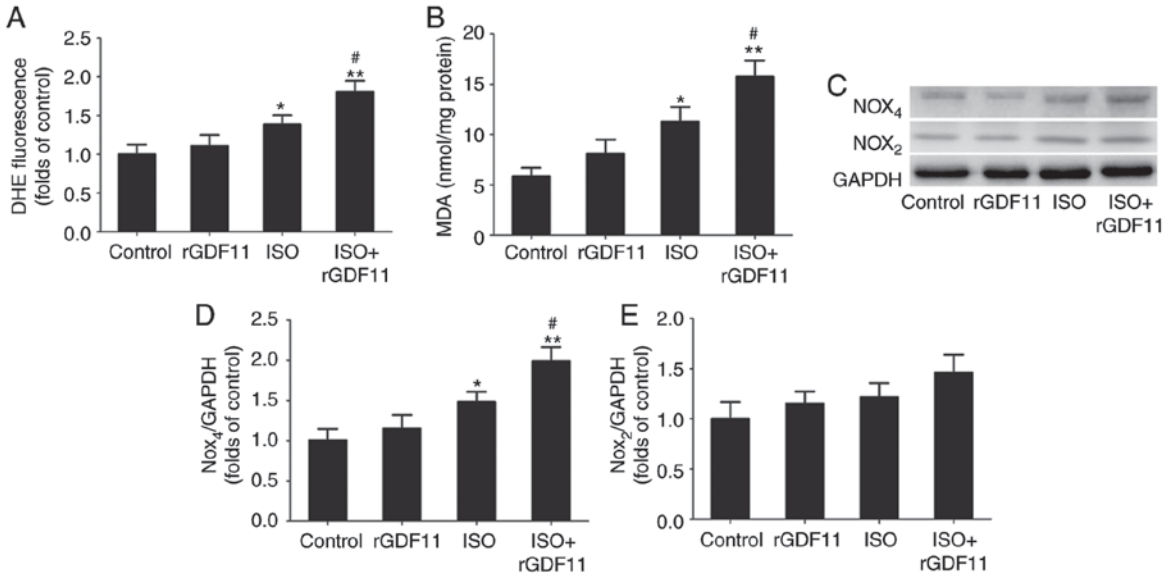

Figure 5. GDF11 increases ISO-induced oxidative stress by upregulating Nox4 in H9C2 cells. (A) Levels of reactive oxygen species in H9C2 cells determined by DHE staining. (B) Concentration of MDA in H9C2 cells. (C) Representative western blot and quantitative analyses of (D) Nox4 and (E) Nox2 expression in H9C2 cells. Data are presented as the mean ± standard error of the mean. *P<0.05, **P<0.01 vs. control group; $^{\#}$P<0.05 vs. ISO group. DHE, dihydroethidium; rGDF11, recombinant growth differentiation factor 11; ISO, isoproterenol; MDA, malondialdehyde; Nox, nicotinamide adenine dinucleotide phosphate oxidase.

significantly reduced the LDH release (Fig. 6C) and apoptosis of ISO-treated cells, represented by the decrease in Bax/Bcl-2 protein expression, caspase-3 activity and apoptotic rate in Hoechst 33258 staining (Fig. 6D-G).

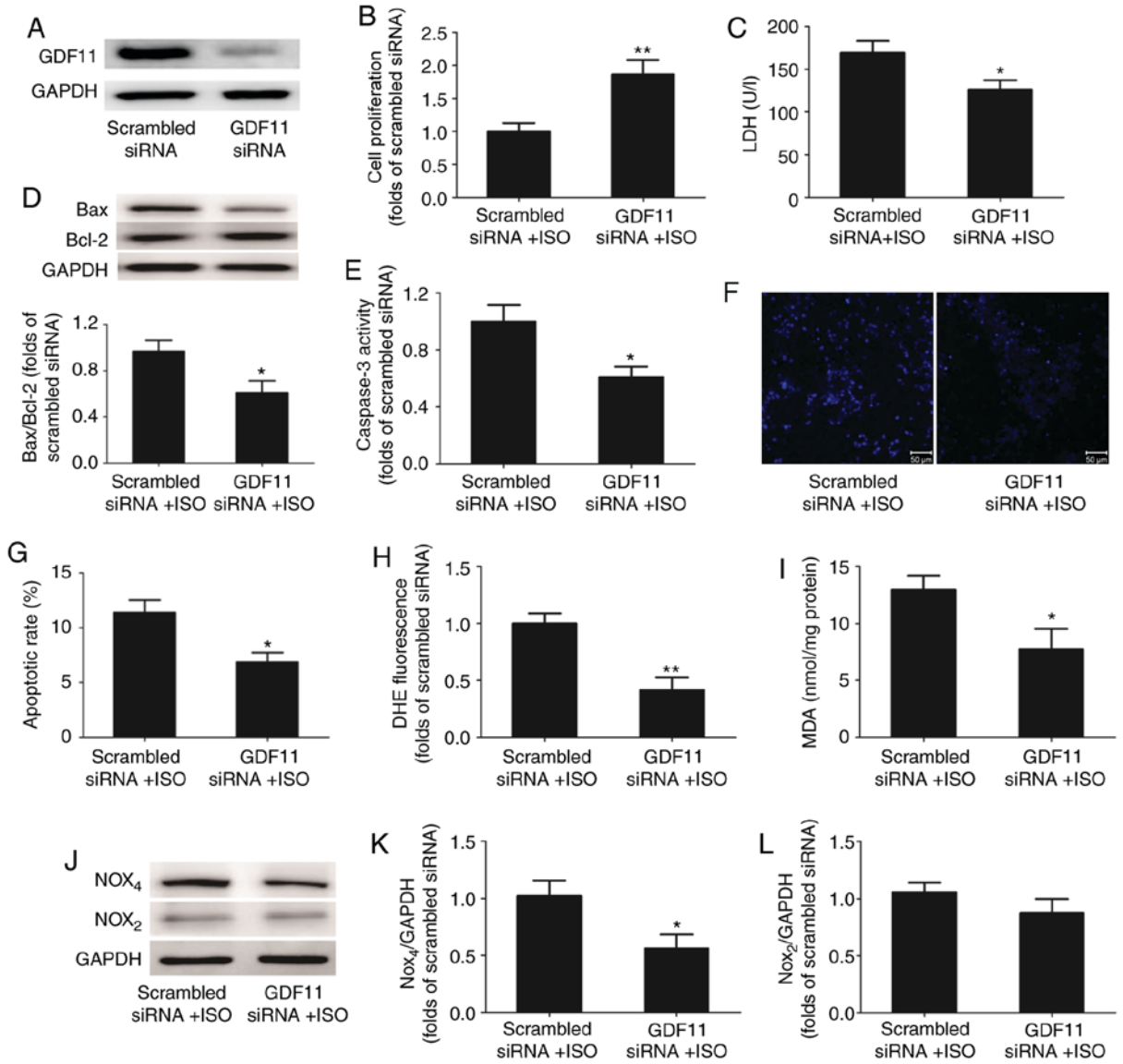

Figure 6. GDF11 knockdown alleviates ISO-induced apoptosis by inhibiting oxidative stress injury. (A) Representative western blot analysis of GDF11 expression in H9C2 cells following transfection with GDF11-specific or scrambled siRNA. (B) Proliferation of H9C2 cells was measured using a Cell Counting Kit-8 assay. (C) Levels of LDH release from H9C2 cells. (D) Representative western blot and quantitative analyses of Bax and Bcl-2 protein expression in H9C2 cells. (E) Caspase-3 activity in H9C2 cells. (F) Representative images and (G) quantitative analysis of apoptotic H9C2 cells stained with Hoechst 33258. (H) Levels of reactive oxygen species in H9C2 cells as determined by DHE staining. (I) Concentration of MDA in H9C2 cells. (J) Representative western blot and quantitative analyses of levels of (K) Nox4 and (L) Nox2 expression in H9C2 cells. Data are presented as the mean ± standard error of the mean. *P<0.05, **P<0.01 vs. scrambled siRNA + ISO group. Bcl-2, B-cell lymphoma 2; Bax, Bcl-2-associated X protein; DHE, dihydroethidium; GDF11, growth differentiation factor 11; ISO, isoproterenol; lactate dehydrogenase; MDA, malondialdehyde; Nox, nicotinamide adenine dinucleotide phosphate oxidase; siRNA, small interfering RNA.

GDF11 knockdown also significantly decreased the concentrations of ROS (Fig. 6H) and MDA (Fig. 6I) in ISO-treated H9C2 cells compared with the control. Additionally, western blot analysis demonstrated that the levels of Nox4 protein expression were downregulated in the GDF11 knockdown group compared with in the scrambled siRNA group; however, the levels of Nox2 expression were not significantly altered (Fig. 6J-L).

Discussion

The present study revealed that the production of GDF11 was increased in ISO-induced rats with HF and ISO-treated H9C2 cells. Furthermore, rGDF11 treatment of H9C2 cells promoted ISO-induced oxidative stress injury by upregulating the levels of Nox4 expression, whereas GDF11 knockdown downregulated the expression of Nox4. These findings suggested that GDF11 may be a potential target in the treatment of HF.

HF is considered to be a progressive and irreversible disease characterized by failure of cardiac pumping, which is induced by cardiac injury and pathological cardiac remodeling, ultimately leading to ischemia, apoptosis and cell necrosis; thus cardiac pump failure is aggravated. HF is known as the terminal pathological manifestation of a variety of organic heart diseases, such as myocardial infarction (MI). MI involves a restriction in the flow of blood and oxygen to the heart, which induces sudden cardiomyocyte loss. This leads to cardiac fibroblasts and activated myofibroblasts promoting post-MI

cardiac remodeling, which contributes to the development of ventricular dysfunction and HF. ISO-induced MI in rats is a widely accepted non-invasive and reliable model for investigating the molecular mechanisms underlying HF (2,3,28). ISO results in non-uniform, predominantly subendocardial myocardial necrosis with subsequent hypertrophy and remodeling, leading to the presentation of HF similar to that observed in patients with MI following the infarction episode (29). In the present study, rats were intraperitoneally injected with 5 mg/kg ISO once daily for 7 days to establish the model of HF. Hemodynamic parameters, including LVSP, ± dp/dt_{max}, LVEDP and HR were measured 4 weeks later to evaluate left ventricular function. The results revealed that ISO treatment induced a significant increase in LVEDP, and a decrease in LVSP and ± dp/dtmax, with no significant alterations in HR. The plasma levels of myocardial injury markers, including LDH, CK and CK-MB, were increased following ISO treatment. Furthermore, the plasma levels of BNP, an important biomarker of HF, were significantly increased following ISO treatment. These results indicated that ISO treatment successfully induced HF, consistent with previous studies (30,31).

Members of the TGF-β superfamily, which are produced and secreted from cardiac myocytes, serve numerous roles in the development and progression of HF by modulating various phenomena, including the differentiation, proliferation and apoptosis of cells (32). For example, it was reported that GDF15, a member of the TGF-β superfamily, exhibited a protective role in an animal model of HF due to its antiapoptotic and antihypertrophic properties (33). Conversely, numerous human studies have reported that the levels of GDF15 expression are positively associated with the severity of HF; thus, GDF15 expression may be regarded as a potential biomarker for the diagnosis, prognosis and/or risk stratification of patients with HF (34,35). In the present study, an ISO-induced rat model of HF was used to determine alterations in the expression of GDF11, a member of the TGF-β superfamily. GDF11 is known as a rejuvenation factor that reverses aging and aging-associated dysfunction in muscles, nerves and the cardiovascular system (20,36,37). Conversely, certain studies determining the age-associated decline of levels of the circulating GDF11 reported that the expression of GDF11 increased with age, inhibiting muscle regeneration rather than promoting rejuvenation (38,39); however, the effects of GDF11 on ISO-induced HF require further investigation. Thus, it was revealed that levels of GDF11 protein and mRNA expression were significantly increased in rat heart tissues following ISO treatment. Of note, the plasma expression levels of GDF11 were markedly increased in the ISO group compared with in the control group; however, this difference was not significant. This result may be due to the high expression GDF11 in a number of organs, including the pancreas, intestine, kidney, skeletal muscle and heart (40,41); therefore, increased myocardial expression of GDF11 induced by ISO may be insufficient to affect plasma GDF11 levels.

To determine the effects of ISO on GDF11 production in cardiomyocytes, H9C2 cells were treated with ISO for 24 h. Compared with control treatment, the ISO group demonstrated significantly increased levels of GDF11 protein and mRNA expression. To investigate the effects of GDF11 on ISO-treated H9C2 cells, rGDF11 was administered to ISO-treated H9C2 cells, inducing a further decrease in proliferation, and increase in the LDH release and the apoptosis of cells. These findings are consistent with those of previous studies reporting that GDF11 did not reduce neonatal rat ventricular myocyte hypertrophy, but instead induced hypertrophy (22), and cardiac and skeletal muscle dysfunction *in vivo* (42). Conversely, the findings from the present study opposed those of a previous report, which revealed that GDF11 modulated Ca^{2+} signaling and the mothers against decapentaplegic homolog family member 2/3 (Smad2/3) pathway to prevent cardiomyocyte hypertrophy (43). The results of the present study indicated that GDF11 aggravated ISO-induced cell damage in HF; however, the molecular mechanisms underlying the role of GDF11 in HF, such as the signaling pathway involved in the pathogenesis of HF, remain unclear.

ISO treatment generates highly cytotoxic ROS, resulting in the peroxidation of membrane phospholipids, inducing marked impairment of the myocardial membrane associated with infarct-like necrosis of the heart muscle (44). Excessive ROS generation also activates various intracellular signaling pathways regulating myocyte survival, apoptosis and cardiac remodeling (45). Additionally, accumulating evidence suggests that Nox, the major source of ROS in the cardiovascular system, is an important downstream effector of the TGF-β signaling pathway, whereas Nox-dependent redox signaling regulates TGF-β/Smad signaling in a feedforward manner (46). Qin *et al* (47) reported that GDF11 overexpression and ROS overproduction was observed in patients with metastatic oral cancer; however, treatment with the antioxidant, N-acetylcysteine, suppressed the GDF11-induced epithelial-mesenchymal transition and migration of tumor cells. Of note, the present study demonstrated that ISO treatment induced oxidative stress injury, reflected by increased ROS and MDA concentrations, which was exacerbated by rGDF11 treatment in ISO-treated H9C2 cells.

The levels of Nox2 and Nox4 expression in H9C2 cells, the major isoforms in cardiomyocytes, were determined via western blot analysis. The results revealed that Nox4 protein levels following ISO treatment were increased compared with in the control group; rGDF11 treatment further upregulated Nox4 expression in the ISO group. No significant alterations in the levels of Nox2 expression were observed. Conversely, siRNA-mediated knockdown of GDF11 downregulated Nox4 expression, suppressing oxidative stress injury and alleviating the ISO-induced apoptosis of H9C2 cells. These findings suggested that GDF11 increased ISO-induced oxidative stress injury by upregulating Nox4 in H9C2 cells, in agreement with the findings of Zhang *et al* (48), in which GDF11 treatment increased the levels of Nox4 protein expression and ROS production in human umbilical vein endothelial cells. Additionally, TGF-β increased the levels of Nox4 expression without affecting Nox1, Nox2 or Nox5 expression in cardiac fibroblasts (49,50).

In conclusion, the present study demonstrated that GDF11 production is increased in ISO-induced rats with HF and ISO-treated H9C2 cells. Furthermore, rGDF11 treatment increased ISO-induced oxidative stress injury by upregulating Nox4 in H9C2 cells, whereas GDF11 knockdown exhibited opposing effects. These findings suggested that GDF11 may be a potential target in the treatment of HF.

Acknowledgements

Not applicable.

Funding

The present study was supported by the project of Science and Technology Research and Development Guidance Plan of Shijiazhuang City (grant no. 171461913).

Availability of data and materials

The datasets used or analyzed during the present study are available from the corresponding author on reasonable request.

Authors' contributions

X-J Z conceived the study, performed research and wrote the manuscript; HT and Z-F S performed research and analyzed data; NL, YJ and ZH conducted the statistical analysis and participated in the critical discussion. All authors read and approved the final manuscript.

Ethics approval and consent to participate

All animal care and experimental procedures were performed according to the Guide for the Care and Use of Laboratory Animals of the US National Institutes of Health (24). The study was approved by the Ethics Committee of Third Hospital of Shijiazhuang [Shijiazhuang, China; no. 054(2018)].

Patient consent for publication

Not applicable.

Competing interests

The authors declare that they have no competing interests.

References

1. Ambrosy AP, Fonarow GC, Butler J, Chioncel O, Greene SJ, Vaduganathan M, Nodari S, Lam CSP, Sato N, Shah AN and Gheorghiade M: The global health and economic burden of hospitalizations for heart failure: Lessons learned from hospitalized heart failure registries. J Am Coll Cardiol 63: 1123-1133, 2014.
2. Tanai E and Frantz S: Pathophysiology of heart failure. Compr Physiol 6: 187-214, 2015.
3. Luedde M, Spehlmann MW and Frey N: Progress in heart failure treatment in Germany. Clin Res Cardiol 107: 105-113, 2018.
4. Peana D and Domeier TL: Cardiomyocyte Ca^{2+} homeostasis as a therapeutic target in heart failure with reduced and preserved ejection fraction. Curr Opin Pharmacol 33: 17-26, 2017.
5. Uchihashi M, Hoshino A, Okawa Y, Ariyoshi M, Kaimoto S, Tateishi S, Ono K, Yamanaka R, Hato D, Fushimura Y, *et al*: Cardiac-specific bdh1 overexpression ameliorates oxidative stress and cardiac remodeling in pressure overload-induced heart failure. Circ Heart Fail 10: e004417, 2017.
6. Zhang S, Lin X, Li G, Shen X, Niu D, Lu G, Fu X, Chen Y, Cui M and Bai Y: Knockout of Eva1a leads to rapid development of heart failure by impairing autophagy. Cell Death Dis 8: e2586, 2017.
7. Sharma NM, Nandi SS, Zheng H, Mishra PK and Patel KP: A novel role for miR-133a in centrally mediated activation of the renin-angiotensin system in congestive heart failure. Am J Physiol Heart Circ Physiol 312: H968-H979, 2017.
8. Patel KP, Xu B, Liu X, Sharma NM and Zheng H: Renal denervation improves exaggerated sympathoexcitation in rats with heart failure: A role for neuronal nitric oxide synthase in the paraventricular nucleus. Hypertension 68: 175-184, 2016.
9. Budi EH, Duan D and Derynck R: Transforming growth factor-β receptors and smads: Regulatory complexity and functional versatility. Trends Cell Biol 27: 658-672, 2017.
10. Heger J, Schulz R and Euler G: Molecular switches under TGFβ signalling during progression from cardiac hypertrophy to heart failure. Br J Pharmacol 173: 3-14, 2016.
11. Goletti S and Gruson D: Personalized risk assessment of heart failure patients: More perspectives from transforming growth factor super-family members. Clin Chim Acta 443: 94-99, 2015.
12. Guo Y, Gupte M, Umbarkar P, Singh AP, Sui JY, Force T and Lal H: Entanglement of GSK-3β, β-catenin and TGF-β1 signaling network to regulate myocardial fibrosis. J Mol Cell Cardiol 110: 109-120, 2017.
13. Yan Z, Shen D, Liao J, Zhang Y, Chen Y, Shi G and Gao F: Hypoxia suppresses TGF-β1-induced cardiac myocyte myofibroblast transformation by inhibiting Smad2/3 and rhoa signaling pathways. Cell Physiol Biochem 45: 250-257, 2018.
14. Anand IS, Kempf T, Rector TS, Tapken H, Allhoff T, Jantzen F, Kuskowski M, Cohn JN, Drexler H and Wollert KC: Serial measurement of growth-differentiation factor-15 in heart failure: Relation to disease severity and prognosis in the valsartan heart failure trial. Circulation 122: 1387-1395, 2010.
15. Morine KJ, Qiao X, York S, Natov PS, Paruchuri V, Zhang Y, Aronovitz MJ, Karas RH and Kapur NK: Bone morphogenetic protein 9 reduces cardiac fibrosis and improves cardiac function in heart failure. Circulation 138: 513-526, 2018.
16. McPherron AC, Lawler AM and Lee SJ: Regulation of anterior/posterior patterning of the axial skeleton by growth/differentiation factor 11. Nat Genet 22: 260-264, 1999.
17. Li H, Li Y, Xiang L, Zhang J, Zhu B, Xiang L, Dong J, Liu M and Xiang G: GDF11 attenuates development of type 2 diabetes via improvement of islet β-cell function and survival. Diabetes 66: 1914-1927, 2017.
18. Yu X, Chen X, Zheng XD, Zhang J, Zhao X, Liu Y, Zhang H, Zhang L, Yu H, Zhang M, *et al*: Growth differentiation factor 11 promotes abnormal proliferation and angiogenesis of pulmonary artery endothelial cells. Hypertension 71: 729-741, 2018.
19. Rochette L, Zeller M, Cottin Y and Vergely C: Growth and differentiation factor 11 (GDF11): Functions in the regulation of erythropoiesis and cardiac regeneration. Pharmacol Ther 156: 26-33, 2015.
20. Loffredo FS, Steinhauser ML, Jay SM, Gannon J, Pancoast JR, Yalamanchi P, Sinha M, Dall'Osso C, Khong D, Shadrach JL, *et al*: Growth differentiation factor 11 is a circulating factor that reverses age-related cardiac hypertrophy. Cell 153: 828-839, 2013.
21. Olson KA, Beatty AL, Heidecker B, Regan MC, Brody EN, Foreman T, Kato S, Mehler RE, Singer BS, Hveem K, *et al*: Association of growth differentiation factor 11/8, putative anti-ageing factor, with cardiovascular outcomes and overall mortality in humans: Analysis of the heart and soul and HUNT3 cohorts. Eur Heart J 36: 3426-3434, 2015.
22. Smith SC, Zhang X, Zhang X, Gross P, Starosta T, Mohsin S, Franti M, Gupta P, Hayes D, Myzithras M, *et al*: GDF11 does not rescue aging-related pathological hypertrophy. Circ Res 117: 926-932, 2015.
23. Schafer MJ, Atkinson E, Vanderboom PM, Kotajarvi B, White TA, Moore MM, Bruce CJ, Greason KL, Suri RM, Khosla S, *et al*: Quantification of GDF11 and myostatin in human aging and cardiovascular disease. Cell Metab 23: 1207-1215, 2016.
24. Bayne K: Revised Guide for the Care and Use of Laboratory Animals available. American Physiological Society. Physiologist 39: 199, 208-11, 1996.
25. Simko F, Bednarova KR, Krajcirovicova K, Hrenak J, Celec P, Kamodyova N, Gajdosechova L, Zorad S and Adamcova M: Melatonin reduces cardiac remodeling and improves survival in rats with isoproterenol-induced heart failure. J Pineal Res 57: 177-184, 2014.
26. Livak KJ and Schmittgen TD: Analysis of relative gene expression data using real-time quantitative PCR and the 2(-Delta Delta C(T)) method. Methods 25: 402-408, 2001.
27. Patil AS, Singh AD, Mahajan UB, Patil CR, Ojha S and Goyal SN: Protective effect of omeprazole and lansoprazole on β-receptor stimulated myocardial infarction in Wistar rats. Mol Cell Biochem, 2019.

28. Wong ZW, Thanikachalam PV and Ramamurthy S: Molecular understanding of the protective role of natural products on isoproterenol-induced myocardial infarction: A review. Biomed Pharmacother 94: 1145-1166, 2017.
29. Teerlink JR, Pfeffer JM and Pfeffer MA: Progressive ventricular remodeling in response to diffuse isoproterenol-induced myocardial necrosis in rats. Circ Res 75: 105-113, 1994.
30. Wang JJ, Rau C, Avetisyan R, Ren S, Romay MC, Stolin G, Gong KW, Wang Y and Lusis AJ: Genetic dissection of cardiac remodeling in an isoproterenol-induced heart failure mouse model. PLoS Genet 12: e1006038, 2016.
31. Mohamed SS, Ahmed LA, Attia WA and Khattab MM: Nicorandil enhances the efficacy of mesenchymal stem cell therapy in isoproterenol-induced heart failure in rats. Biochem Pharmacol 98: 403-411, 2015.
32. Morikawa M, Derynck R and Miyazono K: TGF-β and the TGF-β Family: Context-dependent roles in cell and tissue physiology. Cold Spring Harb Perspect Biol 8: a021873, 2016.
33. Xu J, Kimball TR, Lorenz JN, Brown DA, Bauskin AR, Klevitsky R, Hewett TE, Breit SN and Molkentin JD: GDF15/MIC-1 functions as a protective and antihypertrophic factor released from the myocardium in association with SMAD protein activation. Circ Res 98: 342-350, 2006.
34. Meijers WC, van der Velde AR, Muller Kobold AC, Dijck-Brouwer J, Wu AH, Jaffe A and de Boer RA: Variability of biomarkers in patients with chronic heart failure and healthy controls. Eur J Heart Fail 19: 357-365, 2017.
35. Wollert KC, Kempf T and Wallentin L: Growth differentiation factor 15 as a biomarker in cardiovascular disease. Clin Chem 63: 140-151, 2017.
36. Katsimpardi L, Litterman NK, Schein PA, Miller CM, Loffredo FS, Wojtkiewicz GR, Chen JW, Lee RT, Wagers AJ and Rubin LL: Vascular and neurogenic rejuvenation of the aging mouse brain by young systemic factors. Science 344: 630-634, 2014.
37. Sinha M, Jang YC, Oh J, Khong D, Wu EY, Manohar R, Miller C, Regalado SG, Loffredo FS, Pancoast JR, *et al*: Restoring systemic GDF11 levels reverses age-related dysfunction in mouse skeletal muscle. Science 344: 649-652, 2014.
38. Egerman MA, Cadena SM, Gilbert JA, Meyer A, Nelson HN, Swalley SE, Mallozzi C, Jacobi C, Jennings LL, Clay I, *et al*: GDF11 increases with age and inhibits skeletal muscle regeneration. Cell Metab 22: 164-174, 2015.
39. Rodgers BD and Eldridge JA: Reduced circulating GDF11 is unlikely responsible for age-dependent changes in mouse heart, muscle, and brain. Endocrinology 156: 3885-3888, 2015.
40. Walker RG, Poggioli T, Katsimpardi L, Buchanan SM, Oh J, Wattrus S, Heidecker B, Fong YW, Rubin LL, Ganz P, *et al*: Biochemistry and biology of GDF11 and myostatin: Similarities, differences, and questions for future investigation. Circ Res 118: 1125-1142, 2016.
41. Jamaiyar A, Wan W, Janota DM, Enrick MK, Chilian WM and Yin L: The versatility and paradox of GDF 11. Pharmacol Ther 175: 28-34, 2017.
42. Zimmers TA, Jiang Y, Wang M, Liang TW, Rupert JE, Au ED, Marino FE, Couch ME and Koniaris LG: Exogenous GDF11 induces cardiac and skeletal muscle dysfunction and wasting. Basic Res Cardiol 112: 48, 2017.
43. Duran J, Troncoso MF, Lagos D, Ramos S, Marin G and Estrada M: GDF11 modulates Ca^{2+}-dependent smad2/3 signaling to prevent cardiomyocyte hypertrophy. Int J Mol Sci 19: E1508, 2018.
44. Mukherjee D, Roy SG, Bandyopadhyay A, Chattopadhyay A, Basu A, Mitra E, Ghosh AK, Reiter RJ and Bandyopadhyay D: Melatonin protects against isoproterenol-induced myocardial injury in the rat: Antioxidative mechanisms. J Pineal Res 48: 251-262, 2010.
45. Fan D, Yang Z, Liu FY, Jin YG, Zhang N, Ni J, Yuan Y, Liao HH, Wu QQ, Xu M, *et al*: Sesamin protects against cardiac remodeling via Sirt3/ROS pathway. Cell Physiol Biochem 44: 2212-2227, 2017.
46. Samarakoon R, Overstreet JM and Higgins PJ: TGF-β signaling in tissue fibrosis: Redox controls, target genes and therapeutic opportunities. Cell Signal 25: 264-268, 2013.
47. Qin X, Kuang H, Chen L, Wei S, Yu D and Liang F: Coexpression of growth differentiation factor 11 and reactive oxygen species in metastatic oral cancer and its role in inducing the epithelial to mesenchymal transition. Oral Surg Oral Med Oral Pathol Oral Radiol 123: 697-706, 2017.
48. Zhang YH, Cheng F, Du XT, Gao JL, Xiao XL, Li N, Li SL and Dong DL: GDF11/BMP11 activates both smad1/5/8 and smad2/3 signals but shows no significant effect on proliferation and migration of human umbilical vein endothelial cells. Oncotarget 7: 46832, 2016.
49. Cucoranu I, Clempus R, Dikalova A, Phelan PJ, Ariyan S, Dikalov S and Sorescu D: NAD(P)H oxidase 4 mediates transforming growth factor-beta1-induced differentiation of cardiac fibroblasts into myofibroblasts. Circ Res 97: 900-907, 2005.
50. Chan EC, Peshavariya HM, Liu GS, Jiang F, Lim SY and Dusting GJ: Nox4 modulates collagen production stimulated by transforming growth factor β1 in vivo and in vitro. Biochem Biophys Res Commun 430: 918-925, 2013.